Journal of Scientific & Industrial Research
Vol. 85, June 2026, pp. 531-537
DOI: 10.56042/jsir.v85i6.23058

Design and Implementation of a Screen-Printed Resistive-Ink Microwave Absorber for X-Band Communication Systems

Avinash[1], Nisha Gupta[2], Shivaji Sinha[3]*, Jatin Gaur[1,4] & Mritunjay Rai[5]

[1]Electronics and Communication Engineering, Bharati Vidyapeeth's College of Engineering, New Delhi, India
[2]Electronics and Communication Engineering, Birla Institute of Technology, Mesra, Ranchi, Jharkhand, India
[3]Department of Electronics and Communication Engineering, JSS University, Noida, India
[4]Electronics and Communication Engineering, National Institute of Technology, New Delhi, India
[5]Electrical and Electronics Engineering, Shri Ramswaroop Memorial University, Barabanki, India

Received 24 August 2025; revised 01 July 2026; accepted 03 August 2026

The design, and system performance evaluation of a flexible Electromagnetic (EM) wave absorber for X-band communication applications are presented in this work. The proposed structure employs a screen-printed, resistive-ink-based Frequency Selective Surface (FSS) on a paper substrate, enabling low-cost and conformal integration. The absorber features a three-layer configuration, with the FSS patterned using resistive ink as the top layer, facilitating efficient attenuation of incident X-band signals. The unit cell has compact dimensions of $0.46\lambda_o \times 0.46\lambda_o \times 0.09\lambda_o$, where λ_o, denotes the free-space wavelength corresponding to the lowest operating frequency of the absorption band. A full simulation made using Computer Simulation Technology (CST) software and high frequency structure simulator (HFSS) software shows a broad fractional bandwidth of 56.17%, which includes the entire X band spectrum. The absorber exhibits consistent performance over different polarization and incident angles, making it effective in Electromagnetic Interference (EMI) applications. The absorber's performance is stable across different polarizations and incident angles, demonstrating its suitability for applications in EMI mitigation in modern communication systems. It is flexible, has broadband functionality, and can be a good choice for future wireless and radar platforms.

Keywords: Absorber, Conductive ink, Flexible substrate, Screen printing, Wideband

Introduction

The rapid growth in invisible pollution, in the form of Electromagnetic (EM) pollution, is a result of the exponential rise in wireless devices. This rise in EM population is creating an increasingly difficult task to manage environmental safety and system performance. To maintain efficient communication in the coexistence of a complex EM environment, a targeted approach is required to achieve higher reliability. With the rise in the number of IoT nodes packed very closely in a small periphery, sharing the EM resources significantly increases the Electromagnetic Interference (EMI). To ensure reliable communication, with good signal strength and minimum data loss, electromagnetic absorbers have provided a practical solution for electromagnetic compatibility.[1,2]

Electromagnetic absorbers, which have the ability to absorb unwanted EM waves, have become a viable option for EMI suppression. However, designing high-performance absorbers remains a challenging task[3], primarily governed by key parameters such as thickness, bandwidth, and absorptivity.[4] Traditional approaches, including multilayer absorbers composed of stacked Frequency Selective Surface (FSS), have demonstrated improved bandwidth performance.[5] However, these solutions often increase the overall thickness of the absorber, which may hinder their integration into compact and conformal systems.[6] To address these constraints, researchers have explored the development of thin, broadband absorbers.[7] One such approach is the use of Circuit Analog Absorbers (CAAs), which utilize periodic arrays of FSS elements to achieve optimal impedance matching and absorption.[8] Variants of CAAs, including those employing lumped elements such as resistive and capacitive components, have been introduced to enhance performance while minimizing thickness.[9–12] Despite their effectiveness, incorporating discrete components into FSS structures introduces complexity in design and fabrication. The wideband properties and mechanical flexibility of the absorber allow to efficiently reduce unwanted electromagnetic

*Author for Correspondence
E-mail: shivaji2006@gmail.com

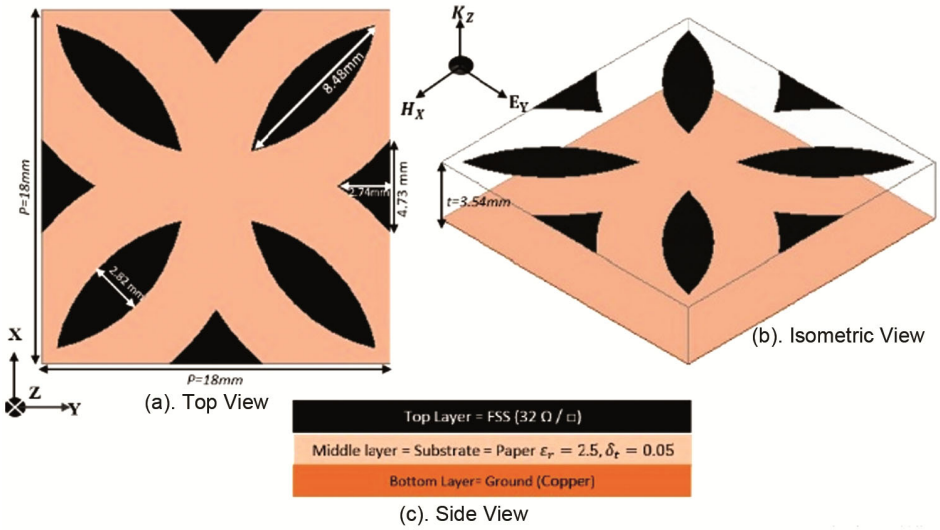


Fig. 1 — Unit cell of the proposed absorber

interference. Recent research suggests the use of resistive-ink based FSS designs,[13,14] which mimic the desired resistive property necessary for absorption without depending on lumped components, making them simpler to fabricate and easier to implement in lightweight and flexible formats. This paper introduces a novel resistive-ink-based absorber for X-band operation to realize broadband absorption in a thin conformal substrate for next generation communication systems.

Design of the proposed Absorber

Geometrical configuration of the proposed absorber, featuring an innovative design tailored to the targeted frequency range is illustrated in Fig. 1. The upper layer, known as the FSS, designed with a novel resistive ink by Bare Conductive®, with a sheet resistance of 32 Ω/□.[15]

The FSS structure combines four triangles positioned at the midpoint of each side of a square patch, with the dimensions of these triangles and ellipses shown in Fig. 1. The FSS structure combines four triangles positioned at the midpoint of each side of a square patch, with the dimensions of these triangles and ellipses. The initial dimensions of the triangular and elliptical shapes were calculated based on the desired frequency range. The unit cell periodicity was first calculated to be less than half the wavelength to prevent grating lobes, followed by separate optimization of the triangle base and height, as well as the ellipse's major and minor axes. After establishing these initial values, comprehensive optimization was performed to finalize the unit cell dimensions. A flexible paper served as a dielectric substrate of dielectric constant 2.2 and loss tangent 0.05, for the proposed absorber which offers versatility appropriate for conformal surface applications. The transmission line approach is used to characterize the electrical properties of the paper substrate. The characterization is done for the complete X-band of the microwave frequency range. The lossy nature of the substrate character is explained by its high loss tangent, which also leads to large dielectric losses in the absorber. The bottom layer comprises copper adhesive tape.

Absorption Mechanism of the Proposed Absorber

How a material interacts with a wave determines whether it reflects, absorbs, or transmits the wave. The main purpose of designing an absorber is to make sure that all the incoming EM waves are absorbed. To obtain the desired absorption performance one must requires an impedance matching among the absorber and the incidence EM wave. The inclusion of copper foil in the proposed absorber acts as a metal ground plane to prevent the EM wave from going through the absorber. Hence, the most important condition is that the character of the EM wave and absorber be identical. The reactive component of the input impedance is very close to 0 Ω at all frequencies and the resistive component is around 377 Ω over a broad frequency range as evident from Fig. 2. Such an impedance behaviour allows the absorber to be used for wideband applications. It is found that the impedance of the absorber at the frequency level at which the highest absorption is obtained

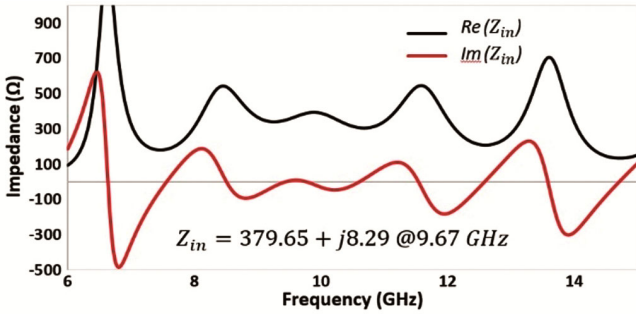


Fig. 2 — Impedance of the absorber

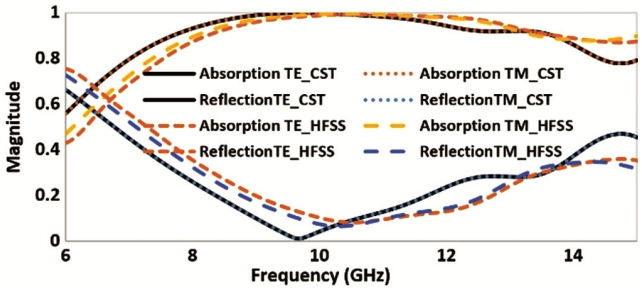


Fig. 3 — Comparison between Simulated absorption and reflection magnitude on CST and HFSS

that is 99.99% at 9.67 GHz, is Z_{in} = 379.65 + j 8.29 Ω, thus the impedance matching error was 0.007.

From the perspective of the input impedance of the proposed absorber and the intrinsic impedance, η_0 of the incident EM wave, magnitude of reflection coefficient is given as Eq. (1)

$$S_{11} = \frac{Z_{in}-\eta_0}{Z_{in}+\eta_0} \quad \ldots (1)$$

The absorption of EM wave by the absorber is calculated[16,17] by Eq. (2),

$$\text{Absorption} = 1 - |S_{11}|^2 - |S_{21}|^2 \quad \ldots (2)$$

Since the transmission is obstructed by the bottom layer of the absorber and hence, $S_{21}\approx 0$, and in final form, absorption magnitude can be given as

$$\text{Absorption} = 1 - |S_{11}|^2 \quad \ldots (3)$$

When the absorber's impedance matches with the incoming EM waves, the waves penetrate the substrate, leading to effective absorption. The simulated absorption and reflection levels are presented in Fig. 3 under direct incidence for both TE and TM modes. It is notable that the reflection coefficient magnitude remains below in the frequency range of 7.68 GHz to 13.68 GHz. Within this band, absorption exceeds 90%, reaching a peak of 99.99% at 9.67 GHz.

Results and Discussion

Due to the unavailability of conductive ink, the proposed absorber has not yet been experimentally verified. However, the upper layer FSS of the suggested absorber can be printed on the top sheet of the dielectric layer using the screen-printing technique. The proposed absorber is designed on 3.54 mm thick substrate whereas, available paper substrate having thickness of 0.177 mm / sheet, a total 20 sheets can be pasted back to back to yield an overall thickness of 3.54 mm. A copper foil is fixed on the last sheet to make ground plane. After the preparation of dielectric substrate and ground plane, the upper FSS layer of the absorber can be fabricated on the top surface of the substrate using a screen-printing technique. Previous studies[13] have reported an absorber fabricated and validated using the same conductive ink, though with different electrical properties. A 40 μm hot lamination film is laminated over the entire absorber as a protective layer. Its small thickness results in minimal influence on the electromagnetic characteristics of the absorber while enhancing resistance to humidity, sweat, and outdoor environmental conditions. To strengthen the credibility of the findings, simulation results were compared using both CST and HFSS, as shown in Fig. 3. The results from both simulation tools are in good agreement, reinforcing the reliability of the proposed design.

Examining the plot of electric field and surface current offers valuable insight into the absorption mechanism. The electric field distribution at three different frequencies on the absorber's top surface as displayed in Fig. 4 are the lower cutoff frequency of 90% absorption bandwidth i.e. 7.68 GHz, the frequency corresponding to maximum absorption i.e. 9.67 GHz and, at the upper cutoff frequency of 90% absorption bandwidth i.e. 13.68 GHz. At 7.68 GHz, the starting frequency of the 90% absorption bandwidth, the electric field originates from the right-side corner ellipses and terminates toward the left-side ellipses and the triangles, creating a resonant effect. At 9.67 GHz, the field is oriented from left to right, with resonance occurring in the left and central parts of the absorber design. At 13.68 GHz, the field moves from left to right, with all elements of the unit cell actively contributing to resonance, demonstrating the effectiveness of the absorber's design. The intensity of the electric field also increases significantly with frequency, and its distribution shows a transition from the edges to the center of the unit cell.

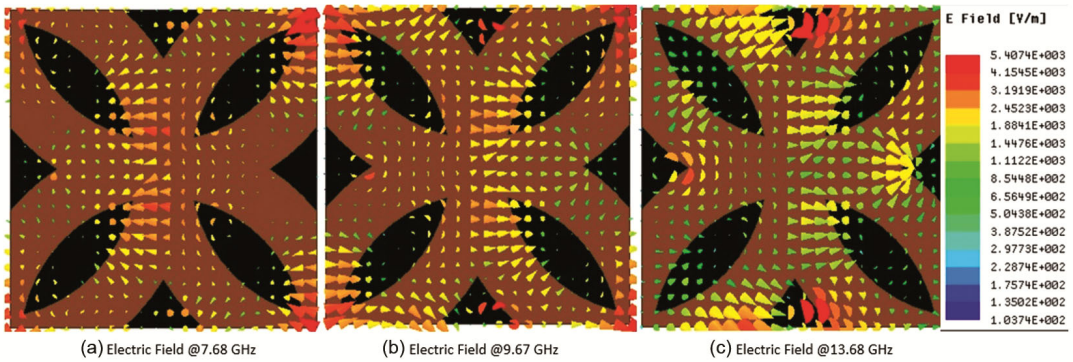


Fig. 4 — Plot of electric field on the top layer of the absorber

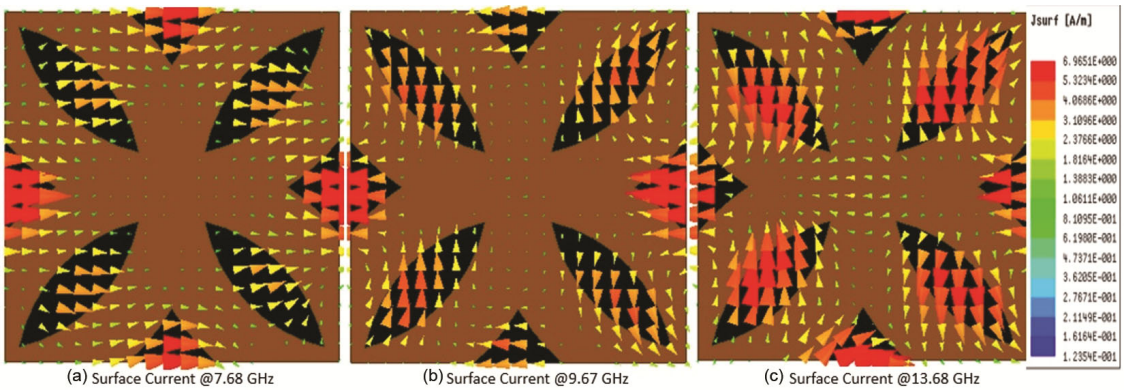


Fig. 5 — Plot of surface current on the top layer of the proposed absorber

The surface current plot on the top layer at the three frequencies 7.68 GHz, 9.67 GHz, and 13.68 GHz as presented in Fig. 5 is providing insight into the absorption mechanism. At 7.68 GHz, the current originates from the left-side triangle, flows through the ellipse at the left corner, and distributes toward the upper and lower triangles, eventually terminating at the right-side triangle via the right-side ellipse. At 9.67 GHz, the current is generated by the upper, lower, and right-side triangles. The current from the upper and lower triangles terminates at the left-side triangle, forming a current loop with the adjacent left-side unit cell. Similarly, the current from the right-side triangle terminates at the right-side ellipse, forming a loop with the adjacent right-side unit cell. This antiparallel current flow results in magnetic resonance, playing a critical role in EM wave absorption. A similar effect, with greater intensity, is observed at 13.68 GHz, further validating the proposed absorber's mechanism.

To achieve polarization insensitivity, it is essential that the FSS structure be symmetric about its axes. Since the proposed absorber possesses a four-fold symmetry about the axis which ensures consistent absorption behavior regardless of polarization, as

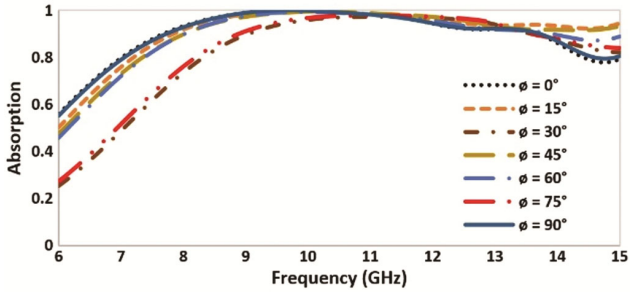


Fig. 6 — Absorption magnitude of the proposed absorber at distinct angle of polarization

demonstrated in Fig. 6, which shows stable absorption performance under different polarization conditions from 0° to 90°, confirming the absorber's inherent polarization insensitivity.

The responses of absorber to oblique incidence across a range of angles are shown in Fig. 7 and Fig. 8, for TE and TM modes respectively. The absorption magnitude at angles of incidence ranging from 0° to 90° at a step size of 15° are displayed in Fig. 7 and show a progressive decrease in absorption as the angle of incidence rises. The angle of incidence affects intrinsic impedance of EM wave. While the absorber's impedance remains constant, the inherent impedance of electromagnetic waves decreases as the angle of

incidence increases. This behavior originates an impedance mismatch between absorber and incident EM waves results deteriorate the absorption magnitude at larger angles. The absorber maintains over 90% absorption up to 45° and above 80% up to 60°, beyond which the absorption level drops significantly. Similarly, for TM mode also intrinsic impedance of the incident EM wave increases with increase in angle of incidence and creates impedance mismatch and hence absorption decreases with angle of incidence. From Fig. 8, it could be observed that the proposed absorber shows absorption more than 90% up to 45° and above 80% up to 60°, beyond which the absorption decreases rapidly.

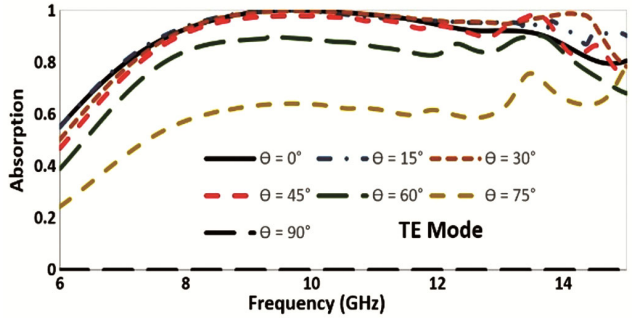


Fig. 7 — Absorption magnitude of the proposed absorber under TE mode at distinct angles of incidence

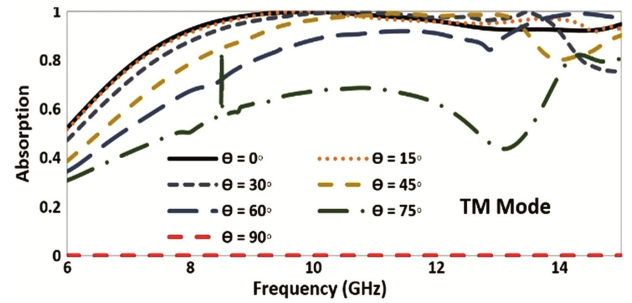


Fig. 8 — Absorption magnitude of the proposed absorber under TM mode at distinct angles of incidence

Effect of Design Parameters

This section presents the effects of key design parameters namely, the unit cell periodicity, substrate thickness, and sheet resistance of the FSS on the behavior of the proposed absorber. The absorber can be fabricated using screen-printing technology[15] however, during fabrication, slight deviations from the optimized parameters may occur. Since the absorption aspects of the proposed absorber are highly sensitive to design parameters, even minor changes can significantly alter its performance. Therefore, it is essential to understand the individual impact of each parameter.

Effect of Periodicity

To begin with, the periodicity 'P' of the geometry of the proposed absorber was varied from 15mm to 20mm in interval of 1 mm, while keeping all other parameters remains unchanged. As the periodicity of the design is increased, the separation linking adjacent unit cells becomes larger. This increase in spacing weakens the near-field electric coupling between adjacent unit cell and reduces the fringing electric fields established across the inter element gaps. The results, shown in Fig. 9, indicate that for periodicities of 15 mm and 16mm, the absorption remains below 80%, whereas values between 17 mm and 20 mm result in absorption exceeding 90% within the desired frequency range.

Effect of Thickness of Substrate

The results of the effect of the thickness of the substrate 't' on the absorption performance are shown in Fig. 10. The thickness was varied from 2.832 mm to 4.248 mm in increments of 0.0354 mm. The separation between the metallic ground plane and the top FSS layer created by a conductive ink, alters the magnetic and electric energy storage in the unit cell with increasing thickness of the substrates. The

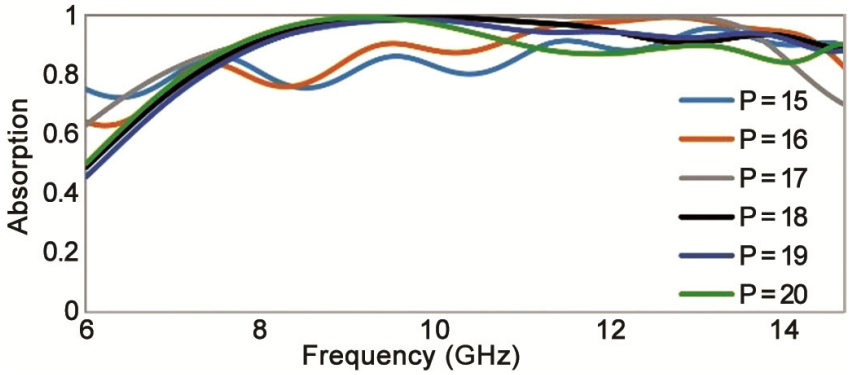


Fig. 9 — Effect of periodicity on the absorption magnitude

Table 1 — Comparison of the proposed absorber with reported absorber

Frequency range (GHz)	Substrate thickness (mm)	Fractional band width (%)	Absorber configuration	Incidence angle	Flexibility[Ref]
7.8 – 12.6	3.2	47	Resistor + CopperFSS + FR4 + Ground	30°	No[9]
7.2 – 12.8	3.4	56	Resistor + CopperFSS + FR4 + Ground	45°	No[12]
8.2 – 13.4	3	48.10	Resistor + CopperFSS + FR4 + Ground	65°	No[13]
7.9 – 12.14	4.6	41	FSS + MagneticRubber + Ground	NA	No[16]
7.88 – 13.03	4.5	49.25	PoP + Acrylic FSS + Groundf	45°	No[17]
7.1 – 13.8	6.0	64	Conductive ribbons + Light polyvinyl chloride + Aluminium	70° (50%Absorption)	Yes[18]
8.44 – 11.10	2.15	27.22	Copper + RO3006 + Aluminium	45°	No[19]
7.68 – 13.68	3.54	56.10	Resistive ink FSS + Paper + Ground	60°	Yes[Proposed]

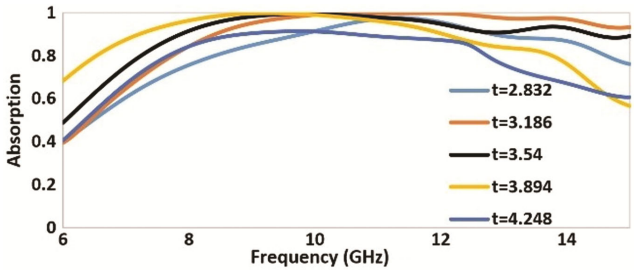


Fig. 10 — Effect of substrate height on the absorption magnitude

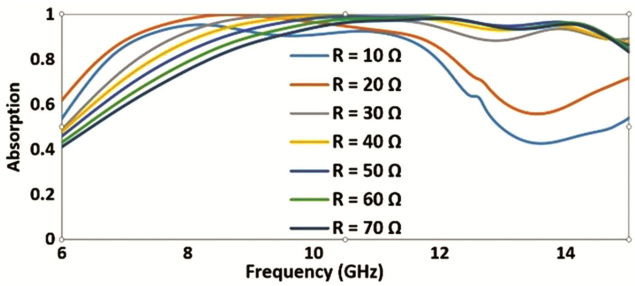


Fig. 11 — Effect of sheet resistance on the absorption magnitude

thickness of the substrate changes the effective inductance due to a greater volume of space in which the magnetic field can be contained and by changing the magnetic coupling between the FSS layer and the ground layer. A new effective capacitance is formed due to the change in the distance between the resonator and ground; this also reduces the capacitive coupling between the resonator and the ground. An increasing thickness of the substrate leads to an increasing absorption which can be detected especially in the mid-frequency area.

Effect of Sheet Resistance

The absorber is fabricated using resistive ink with a sheet resistance of 32 Ω/□, applied to a photo paper substrate via screen printing. The sheet resistance can be adjusted by altering the thickness of the screen print. The sheet resistance 'R' varied in steps of 10 Ω/□ from 10 Ω/□ to 70 Ω/□ in order to investigate this impact. As shown in Fig. 11, both absorption level and bandwidth increase with higher sheet resistance values. However, while increasing sheet resistance broadens the bandwidth, it also reduces peak absorption efficiency due to decreased surface current and impedance mismatch bandwidth increase with higher sheet resistance values.

The pattern was screen-printed using commercially available electric paint from Bare Conductive.[15] Printing several layers of this paint will raise its thickness and change its sheet resistance. However, reprinting multiple layers at the same location may cause ink spreading and mesh pore blockage, compromising the shape and geometry of the pattern and ultimately affecting absorber performance.

The proposed FSS absorber is benchmarked against several previously published designs, with the corresponding performance metrics summarized in Table 1. Among these, the proposed absorber demonstrates notable improvements in Fractional Bandwidth (FBW), overall thickness, and angular stability. Compared to the study by Singh & Gupta[13], it achieves superior bandwidth, fully covering the X-band range (8 GHz to 12 GHz). FBW expressed as a percentage, is determined by taking the ratio of the absolute absorption bandwidth to the corresponding center frequency. A 90% absorption level is adopted as the standard criterion for determining the bandwidth. Although this is accompanied by a slight increase in thickness (0.54 mm), the trade-off is justified by the broader absorption range. Furthermore, unlike the design in Singh & Gupta[13], which requires the manual insertion of a chip resistor during fabrication process that complicates large-scale production, the proposed design avoids the use of such components, enabling a more straightforward and scalable fabrication method.

Conclusions

In conclusion, a flexible, broadband electromagnetic wave absorber operating within the X-band of the microwave spectrum has been proposed. Comprehensive insights into its absorption mechanism and design methodology have been provided. The absorber achieves over 99% absorption efficiency for both TE and TM modes at normal incidence, specifically at 9.67 GHz and across the range of 7.68 GHz to 13.68 GHz, delivering a fractional bandwidth of 56.10% at a threshold of minimum 90% absorption. It features a compact thickness of 3.5 mm, equivalent to 0.09 λ_0. To enhance environmental stability and enable operation in wet conditions, a 0.025 mm thick lamination layer is applied, making the paper-based absorber waterproof and suitable for use in moist environments. The proposed absorber design is compatible with large-scale fabrication through screen printing methods. Due to its full X-band coverage, the proposed absorber is well-suited for satellite and radar communication systems.

References

1 Omoru, Elliot O & Srivastava V M, Switching speed analysis of MOSFET-based absorber integrated antenna for 5G/WiMAX/WLAN, *J Commun*, **18(5)** (2024) 274–282, doi:10.12720/jcm.15.11.833-840.

2 Anum A, Ali T, Akbar S, Obaid I, Anjum M J, Draz U & Shaheen M, Angle adjustment for vertical and diagonal communication in underwater sensor, *Int J Adv Comput Sci Appl* (IJACSA), **11(1)** (2020) 604–616, doi:10.14569/IJACSA.2020.0110175.

3 Landy N I, Sajuyigbe S, Mock J J, Smith D R, & Padilla W J, Perfect metamaterial absorber, *Phys Rev Lett*, **100(20)** (2008) 207402, doi: https://doi.org/10.1103/PhysRevLett.100.207402.

4 Tirkey M M & Gupta N, Electromagnetic absorber design challenges, *IEEE Electrmagn Compat*, **8(1)** (2019) 59–65.doi:10.1109/MEMC.2019.8681370.

5 Xiong H, Hong J S, Luo C M & Zhong L L, An ultrathin and broadband metamaterial absorber using multi-layer structures, *J Appl Phys*, **114(6)** (2003) 064109, doi: 10.1063/1.4818318.

6 Tretyakov S, Thin absorbers: operational principles and various realizations, *IEEE Electrmagn Compat*, **5(2) (**2016) 61−66.

7 Shang Y, Shen Z & Xiao S, On the design of single-layer circuit analog absorber using double-square-loop array, *IEEE Trans Antennas Propag*, **61(12)** (2013) 6022–6029, doi: 10.1109/TAP.2013.2280836.

8 Nguyen T Q H, Nguyen T K T, Cao T T N, Nguyen H & Bach L G, Numerical study of a broadband metamaterial absorber using a single split circle ring and lumped resistors for X-band applications, *AIP Adv*, **10(3)** (2020) 035326, doi: https/doi.org/10.1063/1.5143915.

9 Sheokand H, Singh G, Ghosh S, Ramkumar J, Ramakrishna S A & Srivastava K V, An optically transparent broadband microwave absorber using interdigital capacitance, *IEEE Antennas Wireless Propag Lett*, **18(1)** (2018) 113–117.

10 Li S, Gao L, Cao X, Li W, Zhang Z & Zhang D, Wideband, thin, and polarization-insensitive perfect absorber based the double octagonal rings metamaterials and lumped resistances, *J Appl Phys*, **116(4)** (2014) 043710, doi: 10.1063/1.4891716.

11 Nguyen T T & Lim S, Design of metamaterial absorber using eight- resistive-arm cell for simultaneous broadband and wide-incidence-angle absorption, *Sci Rep*, **8(1)** (2018) 1–10.

12 Nguyen T T & Lim S, Angle-and polarization-insensitive broadband metamaterial absorber using resistive fan-shaped resonators," *Appl Phys Lett*, **112(2)** (2018) 021605, doi: 10.1063/1.5004211.

13 Singh A & Gupta N, Screen-Printed Wideband Absorber for the X and Ku Bands, *IEEE Trans Electromagn Compat*, 2022 1321−1329, doi: 10.1109/TEMC.2022.3180745.

14 Singh A & Gupta N, Parametric study of an ultrathin flexible wide-band Absorber for K band, *2021 IEEE Int Conf Mobile Networks Wireless Commun (ICMNWC)*, Tumkur, Karnataka, India, 2021, doi: 10.1109/ICMNWC52512.2021.9688395.

15 Electric paint technical data sheet, Available: https://cdn.shopify.com/s/files/1/0520/3669/8292/files/EPtechdatsheet.pdf?v=1615226370

16 Y Cheng, He B, Zhao J & Gong R, Ultra-thin low-frequency broad- band microwave absorber based on magnetic medium and metamaterial, *J Electron Mater*, **46(2**) (2017) 1293–1299.

17 Avinash & Gupta N, "Low-cost electromagnetic absorbers for shield packaging," *IEEE T Comp Pack Man*, **13(3)** (2023) 374–381.

18 Zolfagharypour S, Chegini E & Mighani M, Design of wideband metamaterial absorber using circuit theory for X-band applications, *IET Microw Antennas Propag*, **17(4)** (2023) 292–300, doi:10.1049/mia2.12338.

19 T Huang, Wu X L, He W L & Tong M S, A novel design of X-band microwave absorber based on metamaterial, *2022 IEEE Int Symp Antenna Propag USNC-URSI Radio Sci Meet (AP-S/URSI)*, Denver, CO, USA, 2022, doi: 10.1109/AP-S/USNC-URSI47032.2022.9887080.